

# NJC

Accepted Manuscript



This is an *Accepted Manuscript*, which has been through the Royal Society of Chemistry peer review process and has been accepted for publication.

*Accepted Manuscripts* are published online shortly after acceptance, before technical editing, formatting and proof reading. Using this free service, authors can make their results available to the community, in citable form, before we publish the edited article. We will replace this *Accepted Manuscript* with the edited and formatted *Advance Article* as soon as it is available.

You can find more information about *Accepted Manuscripts* in the [Information for Authors](#).

Please note that technical editing may introduce minor changes to the text and/or graphics, which may alter content. The journal's standard [Terms & Conditions](#) and the [Ethical guidelines](#) still apply. In no event shall the Royal Society of Chemistry be held responsible for any errors or omissions in this *Accepted Manuscript* or any consequences arising from the use of any information it contains.

## COMMUNICATION

## Preparation of self-supported crystalline Merlinoite type zeolite W membranes through vacuum filtration and crystallizations for CO<sub>2</sub>/CH<sub>4</sub> separations

Cite this: DOI: 10.1039/x0xx00000x

Received 00th January 2012,  
Accepted 00th January 2012

DOI: 10.1039/x0xx00000x

www.rsc.org/

**Zeolite W membranes were grown on their seeds pellets prepared *via* straightforward vacuum filtration method followed by crystallization, rendering them to be self-supported. Herein, the feasible application of self-supported zeolite W membranes for CO<sub>2</sub>/CH<sub>4</sub> separation with astonishing CO<sub>2</sub>/CH<sub>4</sub> selectivity was demonstrated.**

### Introduction

Considerable extents of the world's natural gas reserves that have been discovered to date are currently limited in production as a result of separation technology limitation. These gas fields contain a large amount of contaminating gases, mainly CO<sub>2</sub> and H<sub>2</sub>S. With CO<sub>2</sub> appearing as an undesirable impurity of up to 70% concentration in certain natural gas wells<sup>1</sup>, separation of CO<sub>2</sub> from natural gas is of utmost interest considering the typical pipeline specifications for natural gas generally require CO<sub>2</sub> concentration of below 3%. Further more, CO<sub>2</sub> reduces the energy content of the natural gas, where it is acidic and corrosive in the presence of water. In this respect, membrane technology could play a significant role in making this process economically viable.

Membranes of various zeolite topologies emerged in the laboratory scale since early 1990s, where their permeation and separation performances were tested<sup>2</sup>. These diverse zeolite membranes which include zeolite T<sup>3,4</sup>, DDR<sup>5,6</sup>, and SAPO-34<sup>7,8</sup> are competent of separating CO<sub>2</sub> from CH<sub>4</sub>. However, very few studies have been reported to date on Merlinoite type zeolite W; it possesses pore channels of 0.31 x 0.35 nm with 8 rings viewed along [100], 0.27 x 0.36 nm with 8 ring viewed along [010], 0.34 x 0.51 nm and 0.33 x 0.33 nm with 8 ring viewed along [001]<sup>9</sup>. These pore structures could allow CO<sub>2</sub> (0.33 nm) molecules to pass through easily while hindering the diffusion of CH<sub>4</sub> (0.38 nm) molecules through the membrane. **Figure 1** displays the framework of Merlinoite structure of zeolite W.

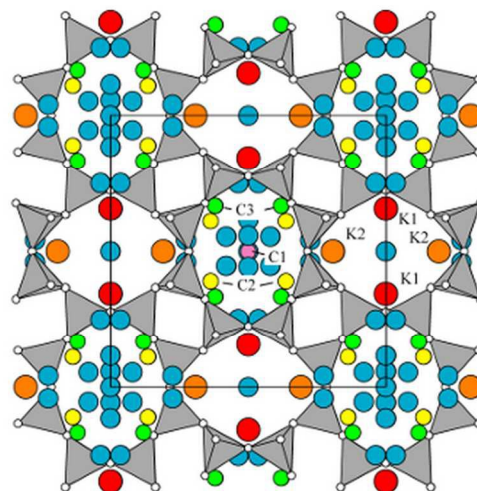


**Figure 1.** The framework of Merlinoite structure. The C1 (pink) site is ~ 30% occupied by Ca<sup>2+</sup> and Na<sup>+</sup>; while C2 (yellow) and C3 (green) are ~ 20% occupied by Na<sup>+</sup>, Ca<sup>2+</sup>, K<sup>+</sup>, and Ba<sup>2+</sup>. The K1 (red) and K2 (orange) sites in the other channels are each ~ 46% occupied mostly by K<sup>+</sup> and minor Ba<sup>2+</sup>. Two fully occupied and six partially occupied H<sub>2</sub>O sites have also been located<sup>10</sup>.

In this present work, a straightforward vacuum filtration method for the formation of zeolite seeds pellets was performed to render them to be self-supported for further crystallizations. Fabrication of self-supported zeolite membranes have been reported previously<sup>11,12</sup>. For instance, Tsapatsis et al.<sup>11</sup> reported the growth of oriented submicron silicalite membrane prepared on composite precursor nano-crystalline silicalite and alumina film *via* secondary growth. Self-supported composite silicalite and alumina films were prepared by initially mixing both silicalite and boehmite suspensions followed by casting them on a casting dish with controlled thickness. The membrane exhibits H<sub>2</sub>/N<sub>2</sub> ideal selectivity of 60 at 150°C and

O<sub>2</sub>/N<sub>2</sub> ideal selectivity of 3.6 at 185°C; where the permeation characteristics are mainly attributed to the preferred orientation of the molecular sieving layer. On the other hand, Wang et al.<sup>12</sup> reported a strategy using polymer-zeolite composite hollow fibers as membrane supports. The zeolite NaA crystals implanted in the polyethersulfone-polymer hollow fibers serve as seeds for the growth of zeolite membrane while strengthening the adhesion of the zeolite membrane. This composite support approach eliminates the seeding process while able to prepare high performance reproducible zeolite membranes.

Notably, self-supported zeolite membrane averts several unfavourable consequences of zeolite membrane preparation. For instance, it could reduce the calcination defects as a result of differences in thermal expansion between the zeolite layer and the support<sup>13, 14</sup>. It also prevents the effects of surface chemistry of the support on zeolite membrane formation. Nonetheless, supported zeolite membranes are still superior to self-supported zeolite membranes in view of their stronger mechanical strength. Despite the cost of zeolite membrane support constituting at least 70% of the total cost of a zeolite membrane<sup>15</sup>, numerous porous supports (such as stainless steel and alumina etc.) have been successfully commercialized in industry where cost is no longer a significant problem. In this work, self-supported zeolite W membranes were tested for both CO<sub>2</sub> and CH<sub>4</sub> separation and their gas separation performances were discussed. For the first time, self-supported inorganic zeolite membranes with attractive CO<sub>2</sub>/CH<sub>4</sub> gas separation performances were demonstrated.

## Results and discussion

Secondary seeded growth is considered an effective approach for the synthesis of an integrated zeolite membrane, plausibly due to a better control of the membrane formation by decoupling both nucleation and growth steps. At present, many efforts have been performed to prepare uniform seed layers as well as strongly adhesive seeds on membrane supports, such as through dip coating, rub coating, step-by-step seeding, etc. Herein, we demonstrated a straightforward vacuum filtration method to create seeds pellet directly as the membrane support to overcome the aforementioned challenges, followed by crystallization to form self-supported zeolite membranes. The membrane fabrication steps are illustrated in **Figure 2**. To the best of our knowledge, the performance of self-supported zeolite W for CO<sub>2</sub>/CH<sub>4</sub> separation has not been reported yet. These zeolite W membranes were characterized for both single gas and equimolar CO<sub>2</sub>/CH<sub>4</sub> gas mixtures separation.

For preparing the self-supported zeolite membranes, the zeolite seed crystals were initially dissolved in de-ionized water to form a uniform suspension. This was followed by vacuum filtration where the resulting seeds powders were moulded into a pellet form. The self-supported zeolite membranes were fabricated through hydrothermal synthesis of the seeds pellet in

the synthesis precursor solutions. The composition of the synthesis precursors was similar to that employed for the synthesis of zeolite seeds with the molar ratio of 1SiO<sub>2</sub>:0.04Al<sub>2</sub>O<sub>3</sub>:0.26Na<sub>2</sub>O:0.09K<sub>2</sub>O:14H<sub>2</sub>O. The hydrothermal synthesis was carried out at 363 K for 45 hours. Subsequently, the resulting membranes were washed with de-ionized water and dried overnight at 353 K to obtain the self-supported zeolite membranes.

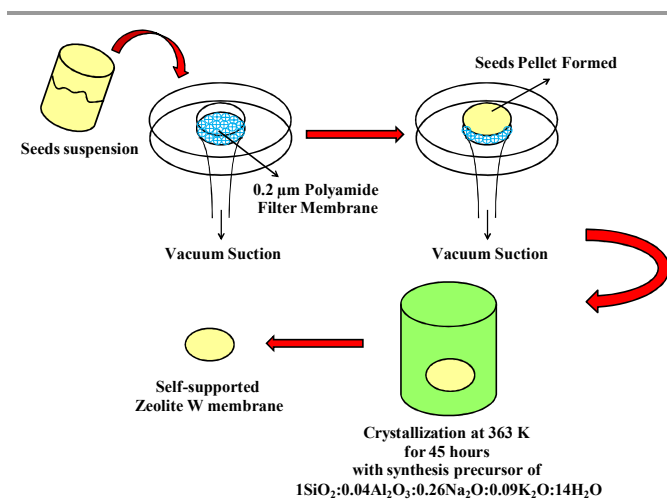


**Figure 2.** Schematic for visualization of self-supported zeolite W membrane fabrication.

The morphological features of zeolite W seed crystals and membranes were characterized by scanning electron microscopy. The synthesized zeolite W seed crystals displayed sizes in the range of ~ 1 μm as shown in **Figure 3a**. These seed crystals exhibit nutshell structure in the outer surfaces of the oval shape seed crystals, which has been observed previously for zeolite W crystals<sup>16</sup>. These crystals were used as seeds for secondary growth to form zeolite W membranes. **Figure 3b** and **3c** show the most representative morphologies observed at the surface of the membranes with both lower magnified and higher magnified zeolite W, approximate to the look of a LEGO structure. Although reported studies<sup>17, 18</sup> have shown zeolite W to resemble those of rod shaped structure, LEGO shape of zeolite W have been obtained in this work. The size of the membrane crystals increased considerably as compared to the size of the seed crystals, which could be related to the re-crystallization of the crystals with the incorporation of zeolite W layer. Despite the whole seed crystals pellet being immersed in the synthesis precursors during hydrothermal treatment, the crystallization of the membrane occurs only on the outer top layer of the pellet forming zeolite W. This is because the seeds pellets are intact and imperforated during the fabrication of the self-supported seeds pellet. As shown in **Figure 3d**, the overall self-supported zeolite W membrane with the seed crystals support displays an average thickness of ~ 130 μm. **Figure 3e** shows the magnified cross sectional area of the zeolite W membrane with an average thickness of ~ 4.5 μm. This thinly grown zeolite W membrane on the outer surface of the seeds

support was probably due to the compact and neatly packed zeolite W seeds during preparation of self-supported seeds pellet which cause the membrane to be thinly crystallized on its outer surface. On the other hand, the XRD peaks of the computer simulated version of Merlinoite type zeolite is shown in **Figure 4i**<sup>9, 19</sup>, with the main peaks represented by asterisks. The XRD patterns of the zeolite seed crystals and membranes are shown in **Figure 4ii** and **4iii**, respectively. The zeolite W seeds pellet exhibited XRD spectrum with the major peaks of  $2\theta = 10.8, 12.3, 16.5, 17.8, 21.0, 21.7, 27.9, 30.3, 32.6, 33.3^\circ$  and while zeolite W membrane pellet exhibited XRD peaks of  $2\theta = 8.8, 10.9, 12.5, 13.5, 17.0, 18.0, 21.7, 22.4, 23.6, 25.0, 27.4, 28.1, 31.6, 32.6, 33.0, 33.5^\circ$ .

**Table 1** shows the  $\text{CO}_2/\text{CH}_4$  separation performance of the self-supported zeolite W membranes (M1-M3) together with the control experiment of self-supported seeds pellet (S). Different batches of self-supported zeolite W membranes denoting M1-M3 showed close values of gas permeances and  $\text{CO}_2/\text{CH}_4$  selectivities, confirming the reproducibility of the membranes. The average single gas permeances of zeolite W self-supported seeds pellet were determined to be  $4.0 \times 10^{-5}$  and  $3.3 \times 10^{-5}$   $\text{mol/m}^2\cdot\text{s}\cdot\text{Pa}$  for  $\text{CO}_2$  and  $\text{CH}_4$ , respectively, indicating the self-supported seeds pellet did not have significant gas separation selectivity. The self-supported zeolite W membranes showed an average  $\text{CO}_2$  and  $\text{CH}_4$  permeances of  $6.1 \times 10^{-7}$   $\text{mol/m}^2\cdot\text{s}\cdot\text{Pa}$  and  $0.082 \times 10^{-7}$   $\text{mol/m}^2\cdot\text{s}\cdot\text{Pa}$ , respectively, with average  $\text{CO}_2/\text{CH}_4$  ideal gas selectivity of 74. Characterizing *via* binary gas permeation, both  $\text{CO}_2$  and  $\text{CH}_4$  showed lower gas permeances with the average  $\text{CO}_2$  and  $\text{CH}_4$  permeances of  $4.4 \times 10^{-7}$   $\text{mol/m}^2\cdot\text{s}\cdot\text{Pa}$  and  $0.069 \times 10^{-7}$   $\text{mol/m}^2\cdot\text{s}\cdot\text{Pa}$ , respectively, and average binary  $\text{CO}_2/\text{CH}_4$  selectivity of 64. It is astonishing to observe that both  $\text{CO}_2$  and  $\text{CH}_4$  showed lower gas permeances in its binary separation as compared to the single gas permeation while presenting indistinguishable separation selectivity. The slowing down of both  $\text{CO}_2$  and  $\text{CH}_4$  gas permeances in binary separation with similar selectivity could be due to the competitive permeation of both  $\text{CO}_2$  and  $\text{CH}_4$  molecules. The  $\text{CO}_2/\text{CH}_4$  binary selectivity which does not deviate too much from the ideal selectivity could be due to the distinct nature of the pore channels of the zeolite W which could effectively separate  $\text{CO}_2$  from  $\text{CH}_4$  molecules. The good separation performance of the zeolite W membranes synthesized may be related to the continuous distribution of the zeolite crystals. In principle, crystals with potentially more homogeneous close packed structure, and therefore less concentration of non-zeolitic pathways, will result in improved gas separation selectivity. The small pore size of zeolite W described earlier could favour the diffusion of  $\text{CO}_2$  (kinetic diameter of 0.33 nm) over  $\text{CH}_4$  (kinetic diameter of 0.38 nm) resulting in a  $\text{CO}_2/\text{CH}_4$  selective membranes. Therefore, the difference in diffusivities between  $\text{CO}_2$  and  $\text{CH}_4$  is the main mechanism by which the separation takes place.

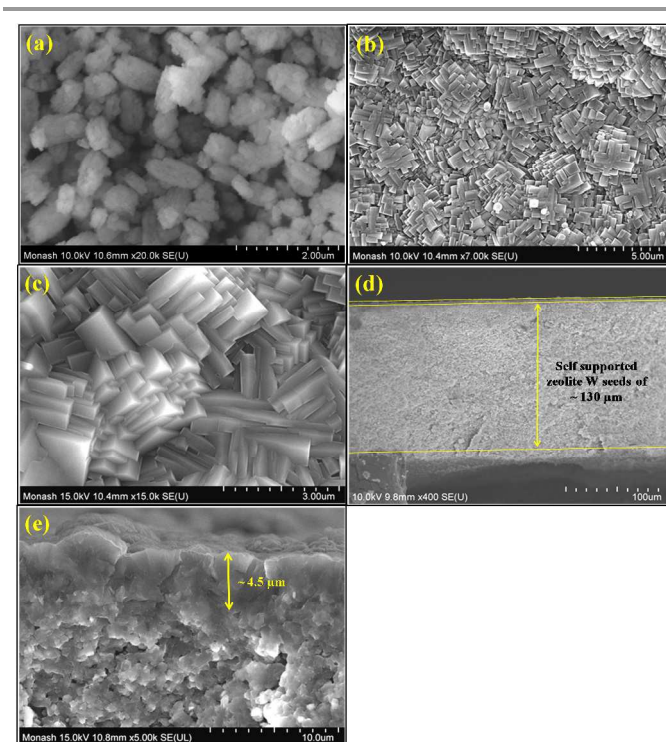


**Figure 3.** (a) Zeolite W seed crystals; (b) lower magnified and (c) higher magnified surface morphology of zeolite W membrane; (d) lower magnified and (e) higher magnified cross-sectional area of self-supported zeolite W membrane

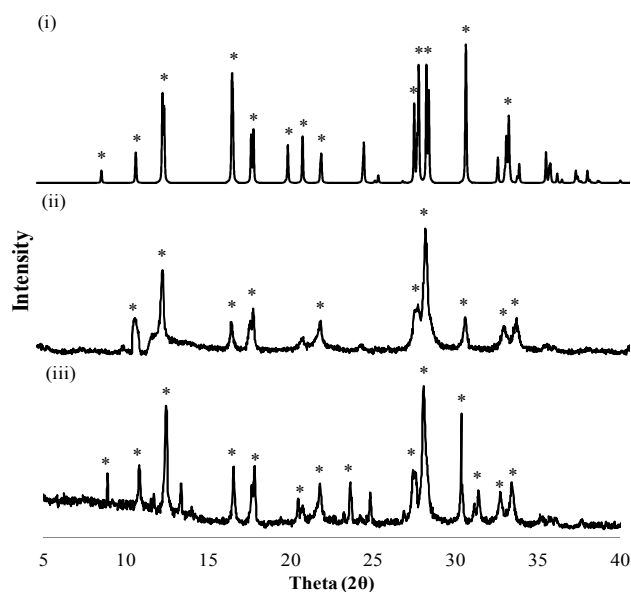


**Figure 4.** (i) Computer simulated version of Merlinoite XRD peaks<sup>9, 19</sup>; XRD patterns of zeolite W (ii) seed crystals and (iii) membrane.



**Table 1.** CO<sub>2</sub> and CH<sub>4</sub> separation performance of self-supported zeolite membranes at 298 K and transmembrane pressure drop of 1 bar.

Self Supported Zeolite W	Permeance (mol/m <sup>2</sup> .s.Pa x 10 <sup>-7</sup> )		Ideal CO <sub>2</sub> /CH <sub>4</sub> Selectivity	Permeance (mol/m <sup>2</sup> .s.Pa x 10 <sup>-7</sup> )		Binary CO <sub>2</sub> /CH <sub>4</sub> Selectivity
	CO <sub>2</sub>	CH <sub>4</sub>		CO <sub>2</sub>	CH <sub>4</sub>	
Seeds pellet, S	400	332	1.2	-	-	-
Membranes, M1	6.2	0.080	77.5	4.6	0.069	66.7
Membranes, M2	5.9	0.087	67.8	4.4	0.068	64.7
Membranes, M3	6.1	0.079	77.2	4.3	0.069	62.3

\* M1-M3 refer to three different batches of self-supported membranes of zeolite W.

The effect of operational temperature on single gas permeation of H<sub>2</sub>, CO<sub>2</sub>, and CH<sub>4</sub> on self-supported zeolite W membrane (M1) is shown in **Figure 5**. Demonstrably, both H<sub>2</sub> and CH<sub>4</sub> showed increasing permeances with increasing temperature; while CO<sub>2</sub> showed gradual increase of permeances up to 373 K followed by a decrease in its permeances subsequently with increasing temperature. On the other hand, H<sub>2</sub>/CH<sub>4</sub> showed steady average selectivity of ~60 while CO<sub>2</sub>/CH<sub>4</sub> showed a decreasing selectivity with increasing operational temperature due to the decreasing CO<sub>2</sub> permeances after 373 K. Despite CO<sub>2</sub> (0.33 nm) molecules showing a higher kinetic diameter as compared to H<sub>2</sub> (0.29 nm) molecules, CO<sub>2</sub> exhibited a slight higher permeances in comparison to H<sub>2</sub>. It is generally known that CO<sub>2</sub> adsorption depends on the Si/Al ratio of zeolite. With zeolite W possessing Si/Al ratio of 3-4, its high Al content will result in larger cationic density, provoking a larger adsorption of CO<sub>2</sub>. Hence, the higher CO<sub>2</sub> permeances as compared to H<sub>2</sub> permeances were due to higher adsorption coverage of CO<sub>2</sub> in zeolitic pore wall which leads to relatively easy diffusion of CO<sub>2</sub> molecules through its pore channels. Therefore, the presence of H<sub>2</sub>/CH<sub>4</sub> selectivities is evidence for the molecular sieving contribution in the zeolite W membrane while CO<sub>2</sub>/CH<sub>4</sub> selectivities is an affirmation of both preferential CO<sub>2</sub> adsorption coupled with molecular sieving effects.

The time stability of the self-supported zeolite W membrane (M1) was investigated using the single gas permeation of both CO<sub>2</sub> and CH<sub>4</sub> gases at 298K with transmembrane pressure drop of 1 bar, shown in **Figure 6**. CO<sub>2</sub> permeance initially with a value of 6.2 x 10<sup>-7</sup> mol/m<sup>2</sup>.s.Pa decreases to 5.3 x 10<sup>-7</sup> mol/m<sup>2</sup>.s.Pa from 0-5 hours and again decreases to 5.0 x 10<sup>-7</sup> mol/m<sup>2</sup>.s.Pa from 5-10 hours and it reaches almost a steady state after 10 hours. They exhibited 14.5% and 19.4% reduction in CO<sub>2</sub> permeances after 5 and 10 hours as compared to initial permeation point. While for CH<sub>4</sub> permeances, it showed a relatively lesser fluctuations with 2.5% reductions in overall, respectively. On the other hand, CO<sub>2</sub>/CH<sub>4</sub> selectivity showed a fascinating value of 77.5 at its early stage of experiments (at 0 hours), followed by a rapid decrease over time until it reaches steady state at 15 hours with selectivity of ~62.4. Since zeolite W demonstrated a preferential CO<sub>2</sub> adsorption, the retardation in CO<sub>2</sub> permeation during 0-10 hours could be reasoned as the saturation and blocking of zeolite W pore channels for effective

molecular diffusion of CO<sub>2</sub> gases. Despite the slowdown of CO<sub>2</sub> permeation with time, the overall CO<sub>2</sub>/CH<sub>4</sub> selectivity was still maintained at ~62. In this case, 3-4 Si/Al ratio of zeolite W membrane showed highest CO<sub>2</sub>/CH<sub>4</sub> selectivity during its initial period of permeation where their separation mechanism was mainly determined by both preferential CO<sub>2</sub> adsorption and molecular sieving. It is self evident that there exist an optimum period for the membrane to demonstrate its highest CO<sub>2</sub>/CH<sub>4</sub> selectivity due to the nature and characteristics of zeolites.

The separation performance of the self-supported zeolite W membranes obtained in this work was compared with that of other zeolite membranes in the Robeson plot shown in **Figure 7**. To calculate the permeability in Barrers for this work, an average membrane thickness of ~ 4.5 μm was used. These data points are well above the present upper bound curves of Robeson plot, showing promising result of the self-supported zeolite W membrane in CO<sub>2</sub>/CH<sub>4</sub> separation. Hence, further research on the self-supported zeolite membranes can be accomplished with current auspicious CO<sub>2</sub> and CH<sub>4</sub> separation performance.

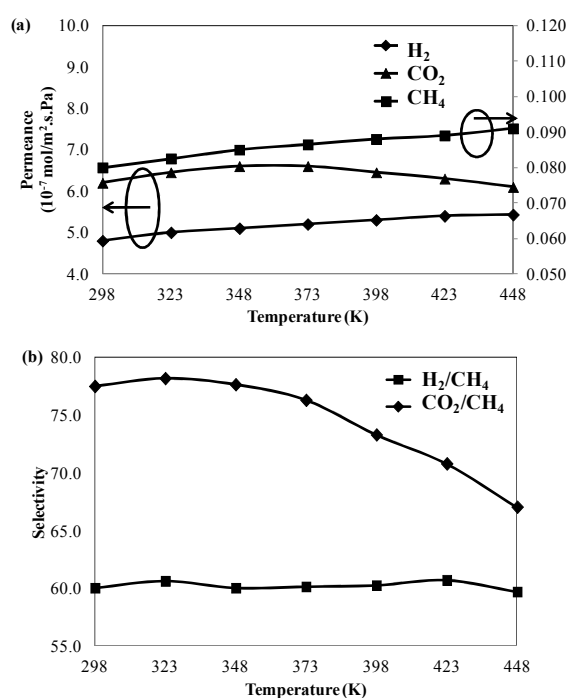


**Figure 5.** (a) Single gas permeation of H<sub>2</sub>, CO<sub>2</sub> and CH<sub>4</sub> gases; and (b) H<sub>2</sub>/CH<sub>4</sub> and CO<sub>2</sub>/CH<sub>4</sub> selectivity; through self-supported zeolite W membrane (M1) as a function of operational temperature at transmembrane pressure of 1 bar.

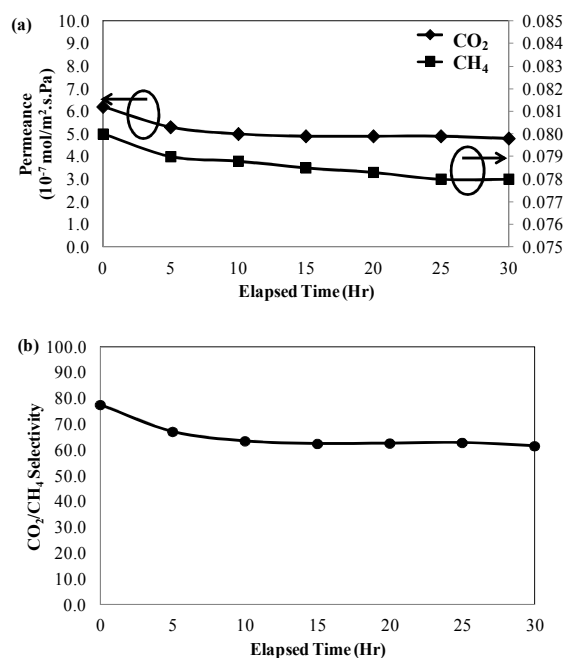


**Figure 6.** (a) Single gas permeation of both CO<sub>2</sub> and CH<sub>4</sub> gases and (b) CO<sub>2</sub>/CH<sub>4</sub> selectivity; through self-supported zeolite W membrane (M1) as a function of elapsed time at 298K and transmembrane pressure of 1 bar.

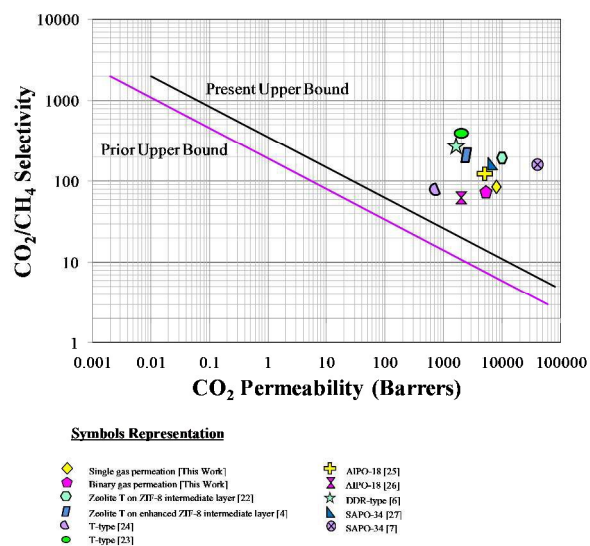


**Figure 7.** Robeson plot for CO<sub>2</sub>-CH<sub>4</sub> mixtures<sup>20, 21</sup>. The symbols represented this work and others from literature were displayed accordingly<sup>4, 6, 7, 22-27</sup>.

## Conclusions

In conclusion, self-supported zeolite W membranes were successfully fabricated through a novel vacuum filtration assisted method and subsequent crystallization. These membranes achieved high CO<sub>2</sub> permeance of  $\sim 6.2 \times 10^{-7}$  mol/m<sup>2</sup>.s.Pa due to the relatively thin membrane layer of  $\sim 4.5$   $\mu$ m. This work demonstrated that it is generally possible to prepare self-supported zeolite membranes with astonishing CO<sub>2</sub> and CH<sub>4</sub> gas selectivity, fueling optimism that self-supported zeolite membranes can be established for natural gas separations.

## Experimental

The synthesis precursor of zeolite W seeds was prepared by mixing corresponding amount of sodium hydroxide (NaOH, Merck), potassium hydroxide (KOH, Merck), sodium aluminate (NaAlO<sub>2</sub>, Sigma Aldrich), fumed silica (SiO<sub>2</sub>, Sigma Aldrich) in de-ionized water with molar composition of 1SiO<sub>2</sub>:0.04Al<sub>2</sub>O<sub>3</sub>:0.26Na<sub>2</sub>O:0.09K<sub>2</sub>O:14H<sub>2</sub>O. The synthesis precursor was aged for 24 hours followed by hydrothermal synthesis at 363 K for 30 hours synthesis period. The hydrothermally treated precursor was collected and subjected to centrifugations with washing steps to recover the seeds prior to usage. Subsequently, a measured weight of zeolite W seeds powder was dissolved in de-ionized water. The zeolite seeds suspension was then poured onto a 0.2  $\mu$ m Nylon membrane (Sterlitech) with vacuum suction to form the seeds pellet. This seeds pellet was then brought into contact with the zeolite precursor solution, similar to the molar composition for preparation of zeolite seeds, at 363 K for 45 hours synthesis period. Lastly, the self-supported zeolite membrane was carefully washed with copious amount of de-ionized water and followed by drying at 353 K for 72 hours.

X-ray diffraction (XRD) patterns were acquired using Bruker D8 Discover with the samples measured from  $2\theta = 5^\circ$  to  $90^\circ$  in  $1^\circ$ /min steps. The morphology of the membranes was inspected through field emission scanning electron microscope (FESEM) collected on Hitachi SU8010. These samples were initially coated with platinum using a sputter coater prior to imaging to mitigate charging. Single gas permeation measurements were carried out at fixed pressure drop of 1 bar at 298 K. The self-supported zeolite W membranes were sealed at its end using adhesive as sealing material between the membrane and the module. This is followed by measurement of the permeate flow rates with a soap film bubble flow meter. The single gas permeation of both CO<sub>2</sub> and CH<sub>4</sub> were determined as a function of permeation time. On the other hand, binary gas permeation was performed with 1:1 CO<sub>2</sub>:CH<sub>4</sub> mixtures with transmembrane pressure drop of 1 bar. The permeation module was purged for at least 1 hour prior to testing and permeates composition were analyzed by gas chromatograph (Agilent 7890A).

### Acknowledgements

We would like to thank the Ministry of Higher Education Malaysia through the Long-term Research Grant Scheme (LRGS) (A/C number 2110226-113-00) for the financial support given.

### Notes and references

a. Low Carbon Economy Group, Chemical Engineering Discipline, School of Engineering, Monash University, 46150 Bandar Sunway, Selangor, Malaysia; Email: chai.siang.piao@monash.edu

b. Department of Chemical Engineering, Lee Kong Chian Faculty of Engineering and Science, Universiti Tunku Abdul Rahman, Jalan Genting Kelang, 53300 Setapak, Kuala Lumpur, Malaysia;

c. Low Carbon Economy Group, School of Chemical Engineering, Engineering Campus, Universiti Sains Malaysia, Seri Ampangan, 14300 Nibong Tebal, Penang, Malaysia.

- H. Lin, E. Van Wagner, R. Raharjo, B. D. Freeman and I. Roman, *Adv. Mater.*, 2006, **18**, 39-44.
- J. Gascon and F. Kapteijn, *Angew. Chem. Int. Edit.*, 2010, **49**, 1530-1532.
- X. Chen, J. Wang, D. Yin, J. Yang, J. Lu, Y. Zhang and Z. Chen, *AIChE J.*, 2013, **59**, 936-947.
- Z. Y. Yeo, P. W. Zhu, A. R. Mohamed and S.-P. Chai, *CrystEngComm*, 2014, **16**, 3072-3075.
- J. Bergh, W. Zhu, F. Kapteijn, J. Moulijn, K. Yajima, K. Nakayama, T. Tomita and S. Yoshida, *Res. Chem. Intermed.*, 2008, **34**, 467-474.
- T. Tomita, K. Nakayama and H. Sakai, *Micropor. Mesopor. Mat.*, 2004, **68**, 71-75.
- M. A. Carreon, S. Li, J. L. Falconer and R. D. Noble, *J. Am. Chem. Soc.*, 2008, **130**, 5412-5413.
- S. Li, J. L. Falconer and R. D. Noble, *J. Membr. Sci.*, 2004, **241**, 121-135.
- C. Baerlocher, L. B. McCusker and D. H. Olson, in *Atlas of Zeolite Framework Types (Sixth Edition)*, eds. C. Baerlocher, L. B. McCusker and D. H. Olson, Elsevier Science B.V., Amsterdam, 2007, pp. 210-211.
- E. Galli, G. Gottardi and D. Pongiluppi, *N Jahrb Mineral Mh*, 1979, **1979**, 1-9.
- M. C. Lovallo and M. Tsapatsis, *AIChE Journal*, 1996, **42**, 3020-3029.
- Q. Ge, Z. Wang and Y. Yan, *J. Am. Chem. Soc.*, 2009, **131**, 17056-17057.
- J. Choi, H.-K. Jeong, M. A. Snyder, J. A. Stoeger, R. I. Masel and M. Tsapatsis, *Science*, 2009, **325**, 590-593.
- E. Kim, J. Choi and M. Tsapatsis, *Micropor. Mesopor. Mat.*, 2013, **170**, 1-8.
- J. Caro, M. Noack and P. Kölsch, *Adsorption*, 2005, **11**, 215-227.
- S. G. Thoma and T. M. Nenoff, *Micropor. Mesopor. Mat.*, 2000, **34**, 301-306.
- A. Bieniok, K. Bornholdt, U. Brendel and W. H. Baur, *J. Mater. Chem.*, 1996, **6**, 271-275.
- A. A. Belhekar, A. J. Chandwadkar and S. G. Hegde, *Zeolites*, 1995, **15**, 535-539.
- Y.-H. Seo, E. A. Prasetyanto, N. Jiang, S.-M. Oh and S.-E. Park, *Micropor. Mesopor. Mat.*, 2010, **128**, 108-114.
- L. M. Robeson, *J. Membr. Sci.*, 1991, **62**, 165-185.
- L. M. Robeson, *J. Membr. Sci.*, 2008, **320**, 390-400.
- Z. Y. Yeo, S.-P. Chai, P. W. Zhu and A. R. Mohamed, *Micropor. Mesopor. Mat.*, 2014, **196**, 79-88.
- Y. Cui, H. Kita and K. Okamoto, *Chem. Commun.*, 2003, 2154-2155.
- X.-L. Zhang, L.-F. Qiu, M.-Z. Ding, N. Hu, F. Zhang, R.-F. Zhou, X.-S. Chen and H. Kita, *Ind. Eng. Chem. Res.*, 2013, **52**, 16364-16374.
- T. Wu, B. Wang, Z. Lu, R. Zhou and X. Chen, *J. Membr. Sci.*, 2014, **471**, 338-346.
- M. L. Carreon, S. Li and M. A. Carreon, *Chem. Commun.*, 2012, **48**, 2310-2312.
- S. Li, J. L. Falconer and R. D. Noble, *Adv. Mater.*, 2006, **18**, 2601-2603.